Bioorganic & Medicinal Chemistry 17 (2009) 7031–7041

Contents lists available at ScienceDirect

Bioorganic & Medicinal Chemistry

journal homepage: www.elsevier.com/locate/bmc

Identification and characterization of novel sirtuin inhibitor scaffolds

Brandi D. Sanders [a,b], Brittany Jackson [a,b], Michael Brent [a,b], Alexander M. Taylor [c], Weiwei Dang [a,e], Shelley L. Berger [a,e], Stuart L. Schreiber [c], Konrad Howitz [d], Ronen Marmorstein [a,b,*]

[a] The Wistar Institute, 3601 Spruce Street, Philadelphia, PA 19104, USA
[b] Department of Chemistry, University of Pennsylvania, 3601 Spruce Street, Philadelphia, PA 19104, USA
[c] Howard Hughes Medical Institute, Broad Institute of Harvard and MIT, Department of Chemistry and Chemical Biology, Harvard University, 12 Oxford Street, Cambridge, MA 02138, USA
[d] ENZO Life Sciences, Inc., 5120 Butler Pike Plymouth Meeting, PA 19462, USA
[e] Department of Cell and Developmental Biology, University of Pennsylvania, Philadelphia, PA 19104, USA

ARTICLE INFO

Article history:
Received 7 May 2009
Revised 23 July 2009
Accepted 26 July 2009
Available online 3 August 2009

Keywords:
Sirtuin
Hst2
SIRT1
Inhibitor

ABSTRACT

The sirtuin proteins are broadly conserved NAD^+-dependent deacetylases that are implicated in diverse biological processes including DNA recombination and repair, transcriptional silencing, longevity, apoptosis, axonal protection, insulin signaling, and fat mobilization. Because of these associations, the identification of small molecule sirtuin modulators has been of significant interest. Here we report on high throughput screening against the yeast sirtuin, Hst2, leading to the identification of four unique inhibitor scaffolds that also inhibit the human sirtuins, SIRT1-3, and are able to inhibit telomeric silencing of yeast Sir2 in vivo. The identified inhibitor scaffolds range in potency from IC_{50} values of 6.5–130 μM against Hst2. Each of the inhibitor scaffolds binds reversibly to the enzyme, and kinetic analysis reveals that each of the inhibitors is non-competitive with respect to both acetyl-lysine and NAD^+ binding. Limited SAR analysis of the scaffolds also identifies which functional groups may be important for inhibition. These sirtuin inhibitors are low molecular weight and well-suited for lead molecule optimization, making them useful chemical probes to study the mechanism and biological roles of sirtuins and potential starting points for optimization into therapeutics.

1. Introduction

The class III family of histone deacetylases (HDACs), or sirtuins, require NAD^+ for the removal of an acetyl moiety from the ε-amino group of lysine residues within protein targets[1,2] to yield the deacetylated protein target, nicotinamide, and 2′-*O*-acetyl-ADP-ribose.[3,4] The founding member of this protein family, *Saccharomyces cerevisiae* Sir2p, was shown to be a limiting factor in yeast aging, as deletion of the SIR2 gene resulted in reduced lifespan,[5] and additional copies of SIR2 resulted in increased yeast replicative lifespan.[6] Furthermore, Sir2p proved to be required for the lifespan extension that results from restricting the caloric intake of yeast cells.[7] Since the sirtuin protein family is broadly conserved,[8] it was also shown that increased expression of sirtuin protein led to increased lifespan in higher organisms such as worms,[9] flies,[10] and mice,[11] and increased longevity due to a calorie restricted diet has been shown in most of these animals to be sirtuin dependent.[10,12] Mammals have seven homologues of the yeast Sir2 protein (SIRT1-7),[13,14] and increased SIRT1 copy number or expression level provides several health benefits in mammals consistent with a reduction is age-related diseases (reviewed in[15]). The most closely related human Sir2p homologue, SIRT1, has been implicated to play a role in a number of age-related human diseases and biological functions such as cell survival, apoptosis, stress resistance, fat storage, insulin production, glucose homeostasis, and lipid homeostasis through direct deacetylation or regulation of its many known in vivo targets including p53, Ku70/Bax, FOXO, PPARγ, PGC1α, UCP2, LXR, and NFκB (reviewed in[15,16]). Although the cellular mechanism by which increased sirtuin activity leads to increased lifespan and/or improvements in the biological functions listed above appears different in each organism, increased sirtuin activity seems to lead to an increase in mitochondrial biogenesis in all organisms, underlying the importance of the metabolic state of the cell for sirtuin activity levels.[16]

The catalytic mechanism by which sirtuin proteins couple NAD^+ cleavage to deacetylation and the mechanism of nicotinamide

Abbreviations: Sir2, silent information regulator number 2; Hst2, homologue of Sir two number 2; SIRT1, silent information regulator two number 1; HTS, high throughput screening; SAR, structure–activity relationship; ADME, absorption distribution metabolism and excretion; sirtuin, homologue of yeast Sir2p.

* Corresponding author. Fax: +1 215 898 0381.
E-mail address: marmor@wistar.org (R. Marmorstein).

0968-0896/$ - see front matter © 2009 Elsevier Ltd. All rights reserved.
doi:10.1016/j.bmc.2009.07.073

inhibition have important implications for Sirtuin regulation by the physiological regulators NAD^+ and nicotinamide, and for development of synthetic regulators of sirtuin proteins. Nicotinamide (**1**), a reaction product and non-competitive inhibitor of Sirtuin proteins,[2,17] has also been shown to be a physiological regulator of this family of proteins.[18] Yeast cells grown in the presence of nicotinamide show a dramatic reduction in silencing, an increase in rDNA recombination, and a shortening of replicative lifespan.[17] Nicotinamide has also been shown to inhibit sirtuin deacetylation in a number of human cell lines.[19] Nicotinamide exerts its inhibitory effect on deacetylation by reacting with a reaction intermediate to reform β-NAD^+ at the expense of deacetylation.[20,21]

Since human sirtuin proteins are involved in a myriad of biological functions directly related to human aging and disease, and because several details of the catalytic mechanism of sirtuin proteins remain to be determined, this class of proteins is an active target for pharmacological small molecule effector design (Fig. 1). In the case of human cancer, SIRT1 inhibitors may prevent the deacetylation of p53 and allow apoptosis in response to cellular damage;[19,22] inhibit silencing of tumor suppressor genes whose DNA is hypermethylated;[23] or increase H4-K16 and H3-K9 acetylation at endogenous promoters to induce gene re-expression in breast and colon cancer cells.[24] The first small molecule sirtuin inhibitors were identified from high throughput yeast phenotypic screens with a Ura3 reporter gene inserted into telomeric regions.[25,26] These inhibitors, sirtinol (**2**) and splitomycin (**3**), have moderate potency (low micromolar) toward Sir2, and while it is not clear exactly where they bind to the enzyme, splitomycin appears to be competitive with the acetyl-lysine substrate. Other sirtuin inhibitors have also been identified such as cambinol (**4**)[27] and the tenovins (**5**)[28] which also have low micromolar potency, decrease tumor cell growth, and are non-competitive with respect to NAD^+ binding. Cambinol is competitive with respect to acetyl-lysine binding while the tenovins are not. In silico screens against the known human SIRT2 structure[29,30] and a model of human SIRT1[31] have also yielded inhibitors with mid to low micromolar potency. Several groups have taken more rational approaches to identifying sirtuin inhibitors. One group screened a library of known kinase inhibitors (ATP mimetics) for their effect on sirtuin activity and identified a potent (sub-micromolar) indole compound, Ro 31-8220 (**6**).[32] Another group purified several molecules from natural sources that were known to have health benefits, but had no known mechanism of action.[33] Finally, a third group tested analogs of polyphenols (putative sirtuin activators).[34] Both of the latter approaches yielded compounds with low micromolar potency. The most successful strategy to date for the identification of sirtuin inhibitors has been in vitro high throughput screening (HTS). Among the compounds identified in this way have been surfactin (**7**)[35] suramin (**8**)[36] and the most potent known sirtuin inhibitors, indole EX527 analogs (**9**, **10**).[37] Surfactin is a large cyclic lipopeptide that is thought to be competitive with NAD^+ binding and may be an effective antimalarial agent through its ability to inhibit *Plasmodium falciparum* Sirtuin. Suramin is very large, and although small molecule analogs of this compound have not been potent sirtuin inhibitors,[38] binding

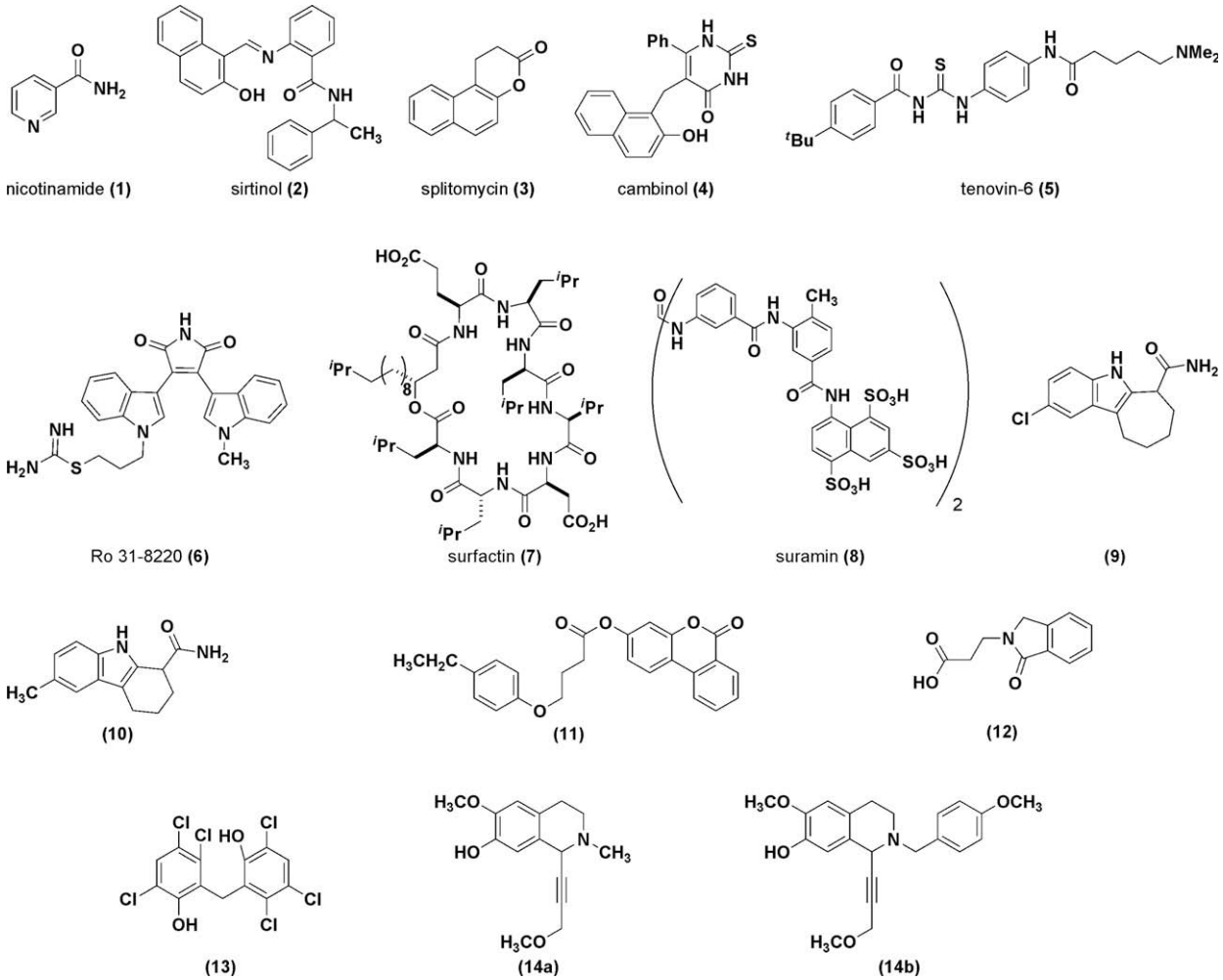

Figure 1. Chemical structure of each of the previously described sirtuin inhibitors and the newly described sirtuin inhibitors identified by HTS.

of the compound to human SIRT5 aided in crystallization of this sirtuin homologue.[39] The indoles are non-competitive with both substrates, are postulated to bind after the release of nicotinamide, and have good ADME characteristics. Structure–activity relationship (SAR) studies of several of the identified inhibitor scaffolds have been performed in an attempt to identify compounds with increased potency and selectivity or more optimal drug-like characteristics with only modest success.[38,40–46]

In order to identify novel sirtuin effector scaffolds, we performed an in vitro high throughput screen of more than 50,000 small molecule compounds against *S. cerevisiae* Hst2. Here, we report four novel compound scaffolds (**11**–**14**) (Fig. 1) that inhibit deacetylase activity of several sirtuin homologues both in vitro and in vivo. To determine which functional groups of these scaffolds were important for deacetylase inhibition, limited SAR data on each of the identified scaffolds was collected. Finally, each of the inhibitor scaffolds was kinetically characterized to gain insight into the binding mode of the inhibitors. The identified inhibitor scaffolds have low micromolar potency and are non-competitive with both substrates. These inhibitor scaffolds may be used for lead molecule optimization to identify more potent and/or selective sirtuin inhibitors with possible therapeutic applications.

2. Results and discussion

2.1. High throughput screen (HTS) for modulators of Hst2

Approximately 50,000 compounds from several Broad Institute small molecule libraries were screened as potential effectors of the *S. cerevisiae* sirtuin, Hst2. The in vitro fluorescently-based screening assay was developed to simultaneously screen for sirtuin inhibitors and activators. Nicotinamide, a reaction product and inhibitor of the sirtuin deacetylase reaction,[2] was added to each reaction well at its approximate IC_{50} concentration in order to inhibit the deacetylase reaction by half. In this way, compounds that inhibited or activated deacetylation through K_m or V_{max} effects or increased the net turnover of the reaction through relief of nicotinamide inhibition could be detected.

The initial HTS identified 74 potential Hst2 effectors, a hit rate of approximately 0.14%. When retested, several of the compounds did not show reproducible effects, inhibited the trypsin assay developer or were autofluorescent at the wavelengths of the experiment (the putative Hst2 activators). These compounds were not pursued further. The remaining four scaffolds, 4-(4-ethyl-phenoxy)-butyric acid 6-oxo-6*H*-benzo[*c*]chromen-3-yl ester (**11**), 3-(1-oxo-1,3-dihydro-isoindol-2-yl)-propionic acid (**12**), hexachlorophene (**13**), 6-methoxy-1-(3-methoxy-prop-1-ynyl) -2-methyl-1,2,3,4-tetrahydro-isoquinolin-7-ol or 6-methoxy-2-(4-methoxy-benzyl)-1-(3-methoxy-prop-1-ynyl)-1,2,3,4,6,7-hexahydro-isoquinolin-7-ol (**14a** or **14b**, respectively) represent novel sirtuin inhibitor scaffolds (Fig. 1). Each of these compounds also showed inhibition of deacetylase activity in an assay using radiolabeled NAD^+ and an unlabeled acetyl-lysine containing peptide (Supplementary Fig. 1), showing that the presence of a fluorescently labeled acetyl-lysine peptide is not required for inhibition. None of these compounds appear to be closely related analogs of either reaction substrate.

2.2. Effect of HTS hits on several sirtuin homologues

Each of the novel inhibitor scaffolds inhibited both Hst2 and the full length human sirtuin, SIRT1, in a dose-dependent manner. The IC_{50} value defines the concentration of inhibitor required to half-saturate the enzyme population under specific assay conditions and is commonly used as a measure of relative inhibitor potency among compounds. Because IC_{50} values are typically used to rank-order the potency of validated hits from HTS,[47] we determined the IC_{50} for each of the inhibitor scaffolds identified in our HTS for both Hst2 and human SIRT1 (Table 1). Several of the newly identified sirtuin inhibitors had low micromolar IC_{50} values (**11**, **12**, **13**) while the remaining inhibitors had IC_{50} values in the mid micromolar range (**14a** and **14b**). Because changes in solution conditions, such as pH, ionic strength, temperature and especially the concentration of substrates can alter the measured IC_{50} value, we determined the IC_{50} value of several previously identified sirtuin inhibitors (**1**–**10**) for comparison, using the same assays conditions that were used for the inhibitors identified in the HTS in this study (Table 1). Significant inhibition for Hst2 or SIRT1 was not observed for several of these inhibitors (**3–5, 7**), under our assay conditions, indicating either that these inhibitors are specific for homologues other than the ones we tested or are not very potent inhibitors under our assay conditions. The previously identified indole compound (**9**)[37] was the most potent inhibitor for both enzymes. Interestingly, several of the scaffolds that we identified (**11**–**13**) were more potent than all previously identified inhibitors tested against Hst2, other than the indoles, suggesting that these scaffolds might be ideal lead molecules for the development of potent and selective sirtuin inhibitors.

Because each of the compounds identified by HTS inhibited both Hst2 and SIRT1, and these sirtuin proteins have very little sequence homology outside of the catalytic core region, these compounds are presumed to bind to the catalytic core region of the proteins and are thus expected to inhibit most sirtuin proteins. To see if this was the case, to determine to what extent other sirtuin homologues are inhibited, and to determine the specificity of the compounds for several sirtuin proteins, we tested the ability of the identified compounds to inhibit a panel of human sirtuin homologues. Scaffold **14** was a potent inhibitor of human SIRT2 and SIRT3, with an apparent IC_{50} value of less than 50 μM. Interestingly, scaffold **11** was a potent inhibitor of SIRT2 but not SIRT3. Scaffolds **12** and **14a** had only weak inhibitory activity against human SIRT2 and SIRT3 (Supplementary Table 1). Human SIRT4 and SIRT7 do not possess in vitro deacetylase activity, and the deacetylase activity of SIRT5 and SIRT6 was too weak under the assay conditions described here to accurately determine the percent of residual enzyme activity. The fact that all of the compounds inhibited SIRT2 and SIRT3 to some extent indicates that these

Table 1
In vitro IC_{50} determination of sirtuin inhibitors identified by HTS and described in the literature for Hst2 and FL SIRT1

Compound	Hst2 IC_{50} (μM)	SIRT1 IC_{50} (μM)
Nicotinamide (**1**)	91 ± 7	250 ± 80
Sirtinol (**2**)	48 ± 11	120 ± 23
Splitomycin (**3**)	>600	>500
Cambinol (**4**)	>1000	>600
Tenovin-6 (**5**)	>100*	~100*
Ro 31-8220 (**6**)	20.0 ± 0.9	25 ± 7
Surfactin (**7**)	>700	>600
Suramin (**8**)	240 ± 70	0.6 ± 0.3
Indole 35 (**9**)	1.3 ± 0.1	0.18 ± 0.02
Indole 2 (**10**)	14.5 ± 0.6	0.64 ± 0.06
11	6.5 ± 1.3	6.0 ± 0.4
12	19.9 ± 0.6	80 ± 5
13	12.5 ± 0.6	34 ± 10
14a	130 ± 4	570 ± 200
14b	260 ± 20	nd

IC_{50} data are reported as the mean and standard deviation of three independent determinations. IC_{50} values that were not determined (nd) or are above the highest concentration tested (>) are indicated. *IC_{50} determination for this compound was limited by a solvent effect on the enzymatic assay although this compound did show inhibitory activity against both enzymes at the concentrations tested.

compounds indeed bind in the catalytic core region of sirtuin proteins to exert their inhibitory effects. The varying potencies of these compounds against different human sirtuin homologues suggests that modification of these lead compounds may increase the selectivity of these compounds for a specific homologue relative to the other human sirtuins.

2.3. Determining inhibitor scaffold binding reversibility

To aid in the determination of the mechanism of inhibition for each newly identified inhibitor scaffold and to assay reversibility of inhibitor binding to the enzyme, we tested whether or not deacetylase inhibition was rapidly reversible, slowly reversible or irreversible. To do this, 100× the normal assay concentration of enzyme was incubated with 10× the IC_{50} concentration of each inhibitor. Then, the enzyme was diluted 100-fold into reaction wells containing both substrates, and the amount of product formation over time was monitored (Fig. 2). If the enzyme inhibitor is rapidly reversible, the progress curve should be linear with a slope equal to about 91% of the control sample since the final inhibitor concentration will be 0.1× IC_{50}, or about 9% inhibited for a well-behaved concentration–response relationship. If the enzyme is irreversible or very slowly reversible on the time scale of the assay, then only about 9% of residual activity will be monitored after the dilution because the initial incubation of the inhibitor was at a concentration of 10× IC_{50}, or ~91% inhibition.[47] For each of the inhibitor scaffolds identified by HTS, the resulting slopes of the progress curves are all within 9% of the slope of the enzyme only sample, within the error of the experiment, and are not near the 9% slope indicative of irreversible inhibitors. Although in some specific cases irreversible inhibitors can be useful pharmacologic lead compounds, most lead molecules that function through enzyme inhibition do so through a simple, reversible binding mechanism.

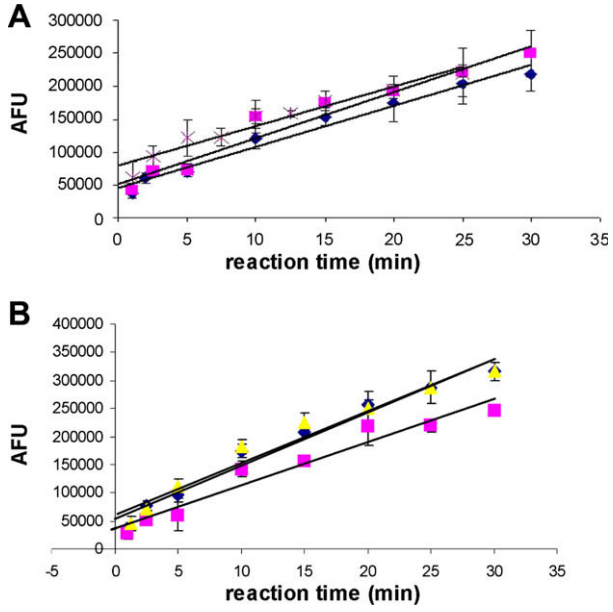

Figure 2. All four HTS inhibitor scaffolds are reversible Hst2 inhibitors. (A) Hst2 reaction time course experiment with both Hst2 alone (blue diamonds) and Hst2 incubated with 10× the IC_{50} concentration of the indicated inhibitor, after a 100-fold dilution. Compounds **14a** (slope 112% of enzyme only control, pink squares) and **13** (slope 85% of enzyme only control, purple asterisks) are reversible inhibitors of Hst2. (B) Hst2 reaction time course experiment with both Hst2 + DMSO (blue diamonds) and Hst2 incubated with 10× the IC_{50} concentration of the indicated inhibitor, after a 100-fold dilution. Compounds **11** (slope 82% of enzyme plus DMSO control, pink squares) and **12** (slope 96% of enzyme plus DMSO control, yellow triangles) are reversible inhibitors of Hst2.

2.4. Limited SAR data for each of the inhibitors identified in HTS

A series of structural analogs of the sirtuin scaffolds identified by HTS were evaluated as inhibitors of Hst2. Following the identification of two compounds with similar scaffolds, **14a** and **14b**, in the initial HTS as Hst2 inhibitors, several analogs of scaffold **14** were synthesized,[48] and their effect as inhibitors of Hst2 was evaluated (Table 2). Compounds **14a** and **14b** differ only in their substitution at the isoquinoline nitrogen, and their structural similarity suggests that these small molecules interact with a similar binding site on the enzyme. The IC_{50} for scaffold **14a** was determined to be about twofold lower than that of scaffold **14b**, implying that the enzyme binding site of this scaffold can accommodate, but does not prefer, the larger 4-methoxybenzyl group of **14b**. Consequently, all of the structural analogs of this scaffold were prepared with a methyl rather than a methoxy-benzyl group on the nitrogen. Analysis of the activity of those analogs makes clear that both

Table 2
Limited SAR analysis of scaffold **14**

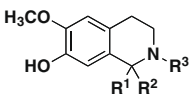

Compound	R^1	R^2	R^3	% Activity at 50 μM	% Activity at 500 μM
7-133	H	H		100	98
7-52		H		100	86
7-56	 (S)	H		96	70
7-57	 (R)	H		97	74
14a	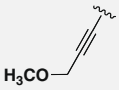	H	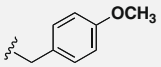	76	5
14b	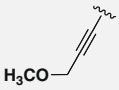	H		92	2
7-128	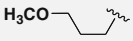	H		99	92
7-129	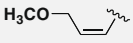	H		97	94
7-123	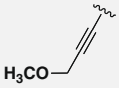			100	100

Data are reported as the percent of residual enzyme activity in the presence of 50 or 500 μM compound relative to the control reaction with no added inhibitor. Data are reported as the average of three independent determinations, standard deviation of the average ⩽ 10%.

the alkyne and ether groups in the R^1 position are absolutely required for inhibitory activity. Varying the ligand in the R^3 position might be effective in the preparation of more potent related compounds, as these data suggest that substituents in this position can be accommodated by the enzyme active site and may impact the binding interaction with the enzyme.

For the remaining scaffolds identified by HTS, commercially available molecules with similar scaffolds were purchased and evaluated for their effect on Hst2 deacetylase activity. None of the analogs of scaffold **11** (Table 3) contained a phenyl group in the R^4 position and none of the analogs were as potent as compound **11**, suggesting that the phenyl group may be important for inhibitor activity especially since compounds 6802623, 7985301, and 6978945 had significantly reduced potency, although there are other differences between the analogs and the originally identified scaffold. The length of the carbon chain included in this scaffold (constituents A and B) may be flexible, as compound 5140108 showed some deacetylase inhibition.

Several analogs of scaffold **13** were also tested for their ability to inhibit deacetylation by Hst2 (Table 4). None of the compounds tested showed significant inhibitory activity against Hst2. The compound with the most inhibitory activity, 97252, had several methyl groups in place of the chloro groups. This seems to indicate that these groups are tolerated in the enzyme active site, but are not ideal for inhibition. The chloro and hydroxyl groups on the originally identified scaffold molecule probably make important interactions in the enzyme binding site and should be explored individually to see which are absolutely required for inhibitory effect and which may be changed in order to generate more potent or selective inhibitors.

Table 3
Limited SAR analysis of scaffold **11** by closely related commercial compounds

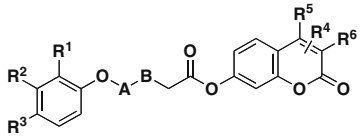

Compound	A	B	R^1	R^2	R^3	R^4	R^5	R^6	% Activity at 50 μM	% Activity at 500 μM
11	CH_2	CH_2	H	H	CH_2CH_3		—	—	<1	<1
5140108	—	—	H	CH_3	H	—	CH_3	H	90	13
6959933	CH_2	CH_2	H	H	OCH_3	—	CH_3	H	93	35
5237467	—	—	H	H	H	—	CH_3	H	91	45
7985301	CH_2	CH_2	CH_3	H	CH_3		—	—	93	49
7988362	CH_2	CH_2	CH_3	H	CH_3	—	CH_3	H	90	51
6802623	CH_2	CH_2	H	H	CH_2CH_3	—	CH_3	H	86	53
6836332	CH_2	CH_2	H	H	CH_3	—	CH_3	H	99	57
6978945	CH_2	CH_2	H	H	OCH_3		—	—	95	58
5366302	CH_2	CH_2	Cl	H	Cl	—	CH_3	H	90	68
53378	CONH	CH_2	H	H	H	—	CH_3	Cl	100	74

Data are reported as the percent of residual enzyme activity in the presence of 50 or 500 μM compound relative to the control reaction with no added inhibitor. Data are reported as the average of three independent determinations, standard deviation of the average ⩽ 10%.

Table 4
Limited SAR analysis of scaffold **13** by closely related commercial compounds

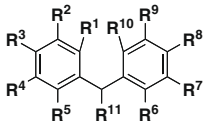

Compound	R^1	R^2	R^3	R^4	R^5	R^6	R^7	R^8	R^9	R^{10}	R^{11}	% Activity at 50 μM	% Activity at 500 μM
13	Cl	Cl	H	Cl	OH	Cl	Cl	H	Cl	OH	H	<1	<1
97252	H	CH_3	OH	CH_3	H	H	CH_3	OH	CH_3	H	H	89	43
97211	H	H	CF_3	H	H	H	H	H	H	H	OH	100	81
72030	H	H	H	H	H	H	H	OH	H	H	H	100	88
56413	H	H	H	NH_2	H	H	NH_2	H	H	H	H	100	100
43909	Cl	H	H	H	H	OH		H	H	H	$NHCOCH_3$	100	100

Data are reported as the percent of residual enzyme activity in the presence of 50 or 500 μM compound relative to the control reaction with no added inhibitor. Data are reported as the average of three independent determinations, standard deviation of the average ⩽ 10%.

Table 5
Limited SAR analysis of scaffold **12** by closely related commercial compounds

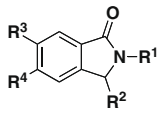

Compound	R^1	R^2	R^3	R^4	IC_{50} (μM)
12	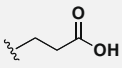	H	H	H	19.9 ± 0.5
39008	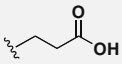	O	Cl	Cl	No inhibition
47054	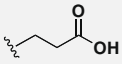	O	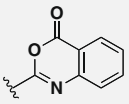	H	No inhibition
42071	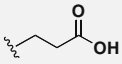	H	NH_2	H	No inhibition
47032	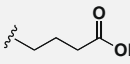	O	H	H	No inhibition
04265	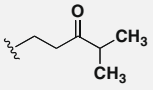	O	H	H	No inhibition
91032		O	H	H	No inhibition
00032	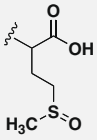	O	H	H	No inhibition

Finally, several analogs of scaffold **12** were tested as potential Hst2 deacetylase inhibitors (Table 5). None of the compounds tested showed any deacetylase activity against Hst2. Generally, most of the analogs of this scaffold contained a second ketone functional group and a constituent in the R^1 position of varying carbon chain length. Because the presence of these groups completely abrogates inhibition, the identity of one or both of these groups in the original scaffold may be critical for Hst2 inhibition.

2.5. Kinetic analysis of inhibition of Hst2 by four inhibitor scaffolds identified in HTS

To determine the mechanism of inhibition of the scaffolds identified by HTS and to gain insight as to where these compounds may bind to the enzyme, inhibition modes were determined by varying each of the substrates with the other maintained at a fixed, saturating concentration (Fig. 3, Table 6). With respect to NAD^+, scaffolds **11**–**13** were best fit to a fully non-competitive inhibition model, with K_i equal to 1.2 ± 0.2, 30 ± 6 and 3.9 ± 0.7 μM, respectively. Scaffolds **14a** was best fit to a fully mixed inhibition model, with K_i equal to 42 ± 17 (α = 2.6) μM. Both of these models imply that the scaffolds bind to the enzyme regardless of whether or not NAD^+ is bound, although with varying affinity in the case of scaffold **14a**, suggesting that the inhibitors bind to a site distinct from the NAD^+ binding site. With respect to the acetyl-lysine substrate, scaffolds **12** and **14a** were best fit to a fully non-competitive inhibition model, with K_i equal to 39 ± 7 and 43 ± 8 μM, respectively. Scaffold **13** was best fit to a fully mixed inhibition model, with K_i equal to 2.5 ± 1.0 (α = 13.4) μM. Finally, scaffold **11** was best fit to a partial non-competitive inhibition model, with K_i equal to 6.3 ± 1.7 μM. Again, each of these models suggests that the newly identified inhibitor scaffolds bind to both the enzyme alone and the enzyme plus acetyl-lysine complex, implying that they bind in a site other than the acetyl-lysine binding site.

2.6. Inhibition of yeast Sir2 activity in vivo by three inhibitor scaffolds identified in HTS

We examined the in vivo efficacy of the inhibitor scaffolds identified in HTS by testing their ability to reduce Sir2 function in the budding yeast *S. cerevisiae*, using an assay that measures Sir2-dependent telomeric silencing. The strain used in this assay contains an insertion of the *URA3* reporter gene at the X core element near *TEL11L* (Fig. 4A). *URA3* encodes orotidine 5-phosphate decarboxylase, which converts 5-fluoroorotic acid (5-FOA) into toxic 5-fluorouracil. Transcriptional silencing facilitated by Sir2 results in resistance to 5-FOA in this strain.[49] As expected, treating cells with a control sirtuin inhibitor, nicotinamide, compromised 5-FOA resistance, demonstrating that inhibition of Sir2 desilences the inserted *URA3* gene (Fig. 4B, row C). This inhibitory effect was evident at 1 mM and reached total inhibition at 5 mM, as judging from similar growth compared to an isogenic strain containing a total *SIR2* gene deletion (Fig. 4B, row D). We tested scaffolds **11**, **12**, and **13** in this assay and observed partial inhibition of Sir2 (reduced 5-FOA resistance) at 500 μM, 1 mM, and 10 μM for scaffolds **11**, **12**, and **13**, respectively. Inhibition of Sir2 neared completion at 40 μM for scaffold **13**, but its toxicity became obvious (Fig. 4B, row A). These results indicate that the inhibitor scaffolds identified in HTS are effective in vivo.

3. Conclusion

The continued development of novel sirtuin inhibitor scaffolds is necessary for the successful development of potent and selective sirtuin probes for further study of sirtuin biology and for development of pharmaceuticals aimed at modulating sirtuin activity for possible therapeutic applications. To address this need, we focused our effector identification efforts on the *S. cerevisiae* Hst2 sirtuin target, an ideal model sirtuin homologue for its ease of overexpression and purification and robust deacetylase activity. Initial HTS hits tend to be general for protein homologues, while further lead molecule optimization can increase both potency and selectivity. Once suitable Hst2 inhibitor scaffolds are identified, they can be tested and potentially optimized using medicinal chemistry against other sirtuin proteins including the human sirtuin homologue, SIRT1.

In this study, we describe the identification of several novel inhibitors against Hst2 that also inhibit human SIRT1-3 through a process of in vitro high throughput screening, initial prioritization of hits by relative potency, characterization of inhibitor binding mode, SAR analysis to identify important functional moieties, kinetic characterization of the mode of compound inhibition, and yeast in vivo studies to show the ability of these compounds to inhibit telomeric silencing. Kinetic studies of the lead compound scaffolds identified here reveal that the mechanism of inhibition is non-competitive or mixed type inhibition relative to both the

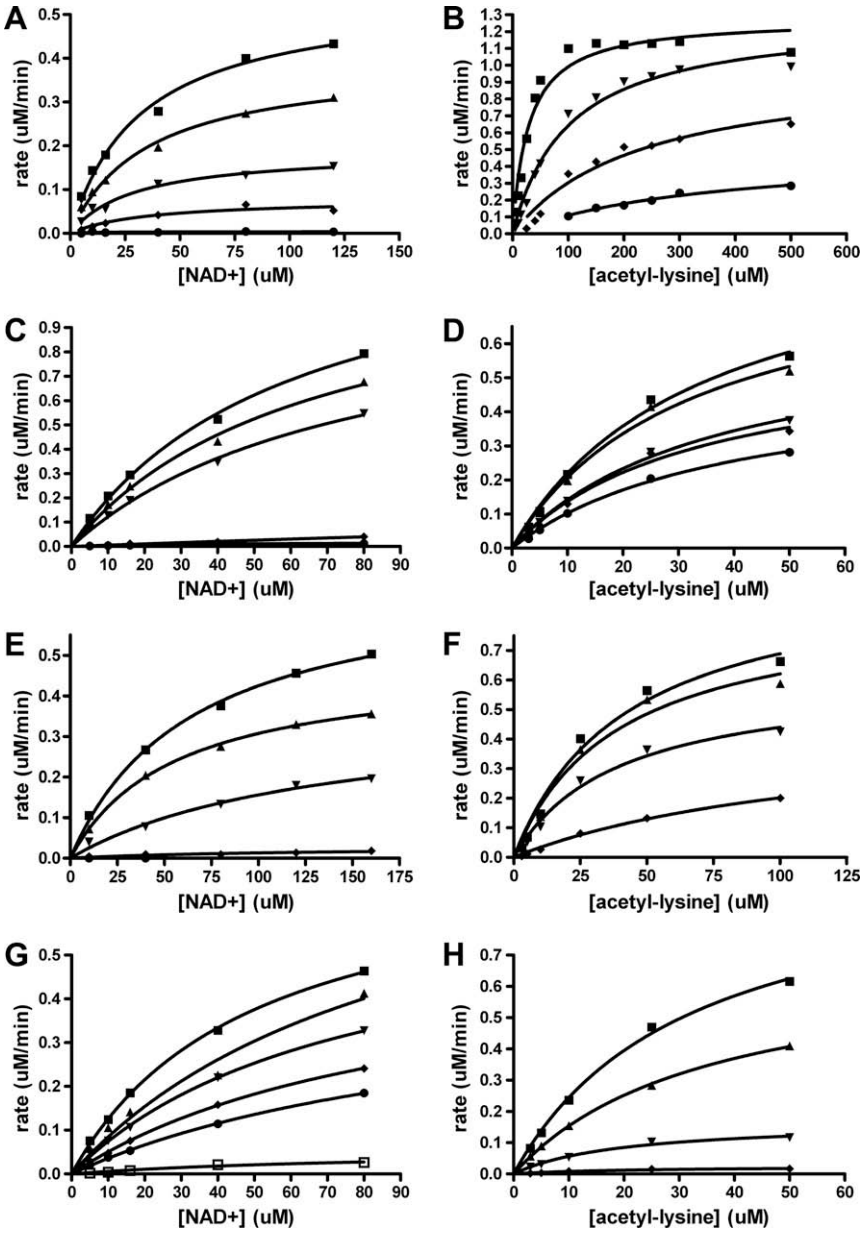

Figure 3. Michaelis–Menten plots of Hst2 in the presence of identified inhibitor scaffolds. (A) Hst2 versus **13** in the presence of varying concentrations of NAD^+. 0 μM **13** (squares), 5 μM **13** (triangles), 7.5 μM **13** (inverted triangles), 10 μM **13** (diamonds), and 15 μM **13** (circles). B) Hst2 versus **13** in the presence of varying concentrations of acetyl-lysine. 0 μM **13** (squares), 10 μM **13** (inverted triangles), 15 μM **13** (diamonds), and 25 μM **13** (circles). C) Hst2 versus **11** in the presence of varying concentrations of NAD^+. 0 μM **11** (squares), 0.5 μM **11** (triangles), 1 μM **11** (inverted triangles), 5 μM **11** (diamonds), and 7 μM **11** (circles). D) Hst2 versus **11** in the presence of varying concentrations of acetyl-lysine. 0 μM **11** (squares), 1 μM **11** (triangles), 5 μM **11** (inverted triangles), 7.5 μM **11** (diamonds), and 15 μM **11** (circles). E) Hst2 versus **12** in the presence of varying concentrations of NAD^+. 0 μM **12** (squares), 25 μM **12** (triangles), 50 μM **12** (inverted triangles), 100 μM **12** (diamonds), and 150 μM **12** (circles). F) Hst2 versus **12** in the presence of varying concentrations of acetyl-lysine. 0 μM **12** (squares), 15 μM **12** (triangles), 30 μM **12** (inverted triangles), and 60 μM **12** (diamonds). G) Hst2 versus **14a** in the presence of varying concentrations of NAD^+. 0 μM **14a** (squares), 25 μM **14a** (triangles), 50 μM **14a** (inverted triangles), 75 μM **14a** (diamonds), 100 μM **14a** (circles), and 200 μM **14a** (empty squares). H) Hst2 versus **14a** in the presence of varying concentrations of acetyl-lysine. 0 μM **14a** (squares), 50 μM **14a** (triangles), 100 μM **14a** (inverted triangles), 200 μM **14a** (diamonds).

acetyl-lysine and NAD^+ substrates. These competition models indicate that the compounds bind both to the free enzyme and to the enzyme/substrate complex, thus implying that the compounds bind to a site distinct from either substrate binding site to inhibit catalysis. Nonetheless, the observation that each of the compounds identified and characterized here inhibit both yeast Hst2 and the human sirtuins SIRT1-3 implies that the target for these compounds is the conserved catalytic domain of these enzymes.

Non-competitive inhibitors act independently of substrate concentration, which makes these inhibitors useful as lead compounds for development as pharmaceutical agents because the in vivo concentration of substrate may be unknown or may vary in diseased cells. Since the sirtuin inhibitors described here were identified through biochemical screens, they may show lower in vivo potency because they have not been selected for their solubility, stability, permeability, localization to a cellular compartment, or accumulation to high concentration inside cells.[28] Similarly, many of the sirtuin inhibitors that have been previously identified are nonspecific,[2,36,46] are of low in vivo potency, or have not been characterized for their in vivo effect on sirtuins. Other sirtuin inhibitors, however, have been shown to have direct in vivo effects. Both sirtinol (**2**) and splitomycin (**3**) can inhibit telomeric silencing in yeast

Table 6
Kinetic properties of the four identified HTS inhibitor scaffolds for Hst2

Scaffold	Substrate	Inhibition mechanism	K_i (μM)	α
11	NAD^+	NC (full)	1.2 ± 0.2	
11	Acetyl-lysine	NC (partial)	6.3 ± 1.7	
12	NAD^+	NC (full)	30 ± 6	
12	Acetyl-lysine	NC (full)	39 ± 7	
13	NAD^+	NC (full)	3.9 ± 0.7	
13	Acetyl-lysine	Mixed (full)	2.5 ± 1.0	13.4
14a	NAD^+	Mixed (full)	42 ± 17	2.6
14a	Acetyl-lysine	NC (full)	43 ± 8	

Data reported are the average of two independent determinations and the standard deviation of the average.

cells.[25,26] Inhibition of SIRT1 by cambinol (**4**) during genotoxic stress leads to hyperacetylation of stress response proteins and promotes cell cycle arrest. Further, treatment of BCL-6 expressing Burkitt lymphoma cells with cambinol (**4**) increased apoptosis and inhibited tumor growth in a Burkitt's lymphoma mouse model.[27] Tenovin-6 (**5**) kills BL2 Burkitt's lymphoma and ARN8 cells in culture and impairs the growth of BL2- and ARN8-derived tumors xenografts.[28] Ro-31-8220 (**6**) inhibits SIRT2 and increases α-tubulin acetylation in A529 cells.[32] Several indole analogs (similar, but not identical to compounds **9** and **10**) reduce TNF-α levels and stimulate adipocyte differentiation.[50] Given that, first, the compounds described here are more potent SIRT1 inhibitors in vitro than the compounds listed above (with the exception of the indole analogs), second, that these compounds inhibit yeast Sir2 in vivo, and third, that the compounds are believed to target the conserved sirtuin core, we conclude that they will likely show some of the same in vivo effects on SIRT1 that were described above.

There are advantages to having several sirtuin inhibitors available. Observing similar effects with several structurally unrelated inhibitors may be an effective way to support the involvement of a sirtuin in a given biological process. In addition, structurally unrelated inhibitors may show benefits in a particular cell line or cancer type. With regard to extending the studies reported here toward therapy, our findings confirm the value of compound scaffolds **11**–**14** as bona-fide sirtuin inhibitors. The advancement of any of the candidate compounds presented here along a drug development path will require a significant investment in medicinal chemistry, preclinical and clinical studies. Nevertheless, these chemical scaffolds along with the limited SAR analysis reported here provide a starting point for the further development of molecules that might be useful for the modulation of aging and for the treatment of age associated disorders, most notably cancer, as inhibitors of the other HDAC families, which share many common protein targets as sirtuins, have potent antitumor activity.[51–53]

4. Experimental

4.1. Protein expression and purification

The 64 residue C-terminal deletion construct of Hst2 (residues 1–294) was purified and expressed as previously described.[54] A plasmid containing full length human SIRT1 (FL SIRT1) was transformed into C41 (DE3) cells (Avidis), expressed overnight at 15 °C by addition of 1 mM IPTG to cell cultures and yielded 6× histidine-tagged SIRT1. Cells were harvested and lysed by sonication in buffer containing 50 mM Tris, pH 7.5, 200 mM NaCl, 5 mM imidizole, 10 mM BME, and 0.1 mg/mL PMSF. Soluble FL SIRT1 was purified by Ni-NTA (Qiagen) in a buffer containing 50 mM Tris, pH 7.5, 300 mM NaCl, 10 mM BME, 5% glycerol, and 30–600 mM imidizole followed by Superdex 200 gel filtration in buffer containing 50 mM Tris, pH 7.5, 150 mM NaCl, and 10 mM BME. FL SIRT1 eluted between the 670 kDa and 158 kDa globular protein standards. Since SIRT1 is known to aggregate after several days at 4 °C, the protein was aliquoted and frozen at −80 °C for use in fluorigenic assays.

A construct of isoform II of SIRT2 with additional residues N-terminal to the SIRT2 gene in a pET30a expression vector was overexpressed as an N-terminal, thrombin-cleavable, His_6-tagged fusion protein in *Escherichia coli* BL21-Gold (DE3) cells, initially grown at 37 °C to exponential phase and induced with 0.5 mM IPTG at 15 °C overnight. Cells harboring SIRT2 were disrupted by sonication in 20 mM Tris, pH 8.5, 500 mM NaCl, and 10 mM BME.

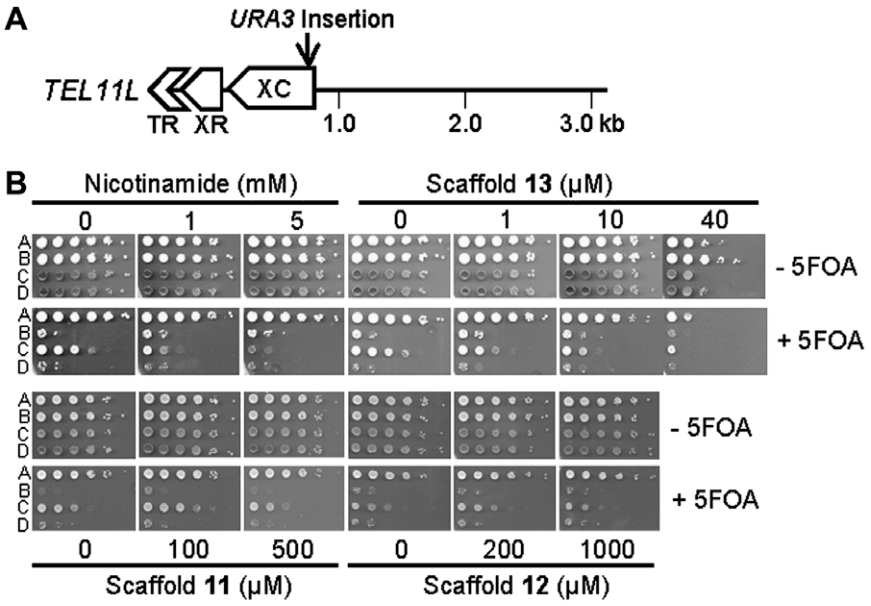

Figure 4. Identified sirtuin inhibitor scaffolds inhibit Sir2 in vivo. (A) Schematic showing the locus of *URA3* insertion for strains used in (B) rows C and D. TR, telomere repeat; XR, X repeat; XC, X core. (B) Telomere silencing assay with sirtuin inhibitors nicotinamide, scaffolds **11**, **12**, and **13** at indicated concentrations. Row A, strain BY4741, *ura3Δ*, a normal growth control on 5-FOA; Row B, strain YWD301, *URA3*, a growth inhibition control on 5-FOA; Row C, strain FEP100-10, *URA3@TEL11L-XC*, the telomere silencing test strain; Row D, strain FEP132, *URA3@TEL11L-XC sir2Δ*, a desilencing control.

Soluble SIRT2 was purified using a combination of Ni-NTA resin, followed by overnight thrombin cleavage, Q sepharose resin and Superdex-200 analytical gel filtration chromatography, where the protein eluted between the 128- and 44-kDa globular protein standards, in a buffer containing 20 mM Tris, pH 8.5, 150 mM NaCl, and 10 mM BME. Human recombinant SIRT3 was purchased from Enzo Life Sciences.

4.2. High throughput screening (HTS)

A high throughput screening protocol based on the BIOMOL SIRT1 Fluorimetric Activity Assay/Drug Discovery Kit (AK-555) was developed. 30 μL of a master mix containing 0.4 μL of the 5 mM Fluor de Lys-SIRT1 deacetylase substrate (KI-177, BIOMOL), 3.2 μL of 1 mM NAD^+ (N1636, Sigma), 0.052 μL of 130 mM nicotinamide (N3376, Sigma), and 26.348 μL of assay buffer (25 mM Tris/Cl, pH 8.0, 137 mM NaCl, 2.7 mM KCl, 1 mM $MgCl_2$) per well was added to each reaction well. 100 nL of either a DMSO control or a compound from the small molecule screening library was added to each well by pinning. To begin the reaction, 10 μL of an enzyme master mix containing 2 μM Hst2 (1–294) (MW = 34859.9 Da) in assay buffer was added to each reaction well. After four hours, a stop/developer solution containing 8 μL of 100 mM nicotinamide, 8 μL of 5× Fluor de Lys Developer II Concentrate (5×) (KI-176, BIOMOL), and 24 μL of assay buffer per well was added to each reaction well. After 45 min, each plate was read on a fluorescence plate reader at an excitation wavelength of 360 nm and an emission wavelength of 460 nm. The nicotinamide and the relatively high concentration of substrates were added to facilitate detection of activators and inhibitors simultaneously. The high throughput screen was carried out at the Broad Institute Chemical Biology Platform's screening facility on ~50,000 small molecules from their ChemDiv3, PKO4, HSCl2, SPBio, and BCB03 libraries, which were selected because they contained commercially available compounds with drug-like structures and known activity, diversity-oriented organic synthesis derived skeletally and stereochemically diverse small molecule analogs of several synthetic pathways, commercially available compounds with known biological activity that are candidates for influencing stem-cell differentiation including COX, NO, adenylate cyclase, and protein kinase effectors, drug-like molecules from the Prestwick and Spectrum commercial libraries, or diverse compound scaffolds synthesized by Broad Chemists and collaborators, respectively. All compounds were screened in duplicate. The fluorescence signal from each well was normalized to the DMSO controls on each 384-well plate and compared to a DMSO control population based on the following equation: $Z = \chi - \mu/\sigma$, where χ is the fluorescence signal of the well, μ is the mean of the control (DMSO) population and σ is the standard deviation of the control population. Generally, compounds that gave fluorescence signals higher than $3Z$ or lower than $-3Z$ were considered hits. Approximately 74 compounds (0.14%) were identified as initial hits and requested as cherry picks. The cherry picked compounds were retested with careful controls to show reproducibility of effect, and rule out autofluorescence, developer inhibition and other assay artifacts.

4.3. IC_{50} determination

The compounds determined to be reproducible and artifact free inhibitors of Hst2 were purchased (**11**, ChemDiv; **12**, TimTec; **13**, Spectrum Chemicals & Laboratory Products) or synthesized (**14**).[48] The purity of the compounds was verified by mass spectrometry (see Supplementary Fig. 2). IC_{50} values were then measured using the same fluorigenic assay described above for Hst2 (160 μM NAD^+, 100 μM Fluor de Lys-SIRT1 deacetylase substrate, 1 μM Hst2, 15 min reaction time) and FL SIRT1 (240 μM NAD^+, 200 μM Fluor de Lys-SIRT1 deacetylase substrate, 1 μM FL SIRT1, and 15 min reaction time). All compounds were solubilized in 25 mM DMSO and diluted for use in the fluorimetric assay of no more than 10% final DMSO concentration. The concentrations of the compounds in the IC_{50} experiment spanned the range of enzyme activity from no inhibition to complete inhibition. The dose–response curves were then fit to one-site competition or sigmoidal-dose–response curves as appropriate in GraphPad Prism (GraphPad Software, La Jolla, CA) and the IC_{50} was determined. Three independent IC_{50} measurements were performed for each compound and the average and standard deviation are reported. In order to directly compare the potency of these compounds to other inhibitors identified in the literature, we also purchased or obtained several known sirtuin inhibitors (sirtinol, Alexis Biochemicals; splitomycin and suramin, BIOMOL International; tenovin-6, Cayman Chemicals; nicotinamide, Sigma; **9** and **10**, Interbioscreen, Ltd; Ro 31820, EMD Chemicals; surfactin, Sigma) and performed IC_{50} experiments using the same assay conditions as described above. Several compounds (cambinol, surfactin and splitomycin) have been shown to be competitive with one of the reaction substrates. Additionally, the IC_{50} values of these compounds also were determined in reaction conditions where the concentration of the competitive substrate was reduced to its approximate K_m value (10 and 45 μM of acetyl-lysine and 16 and 24 μM of NAD^+ for Hst2 and FL SIRT1, respectively).

4.4. Reversibility assay

Each of the inhibitor scaffolds identified in the HTS was tested to determine whether they were reversible, slowly reversible or irreversible inhibitors of Hst2. The reversibility of each compound was identified using the fluorigenic assay described above. First, either the enzyme alone, the enzyme plus DMSO or the enzyme plus 10× the IC_{50} concentration of an identified inhibitor was incubated with 100 μM Hst2 for 30 min. The enzyme, enzyme plus DMSO or enzyme plus inhibitor was then diluted 100-fold into reaction buffer containing the Fluor de Lys-SIRT1 deacetylase substrate and NAD^+ at concentrations equal to their approximate K_m values (25 μM) to initiate the reaction. The reactions were quenched during the linear region of the reaction time course (1–30 min) with 10 mM nicotinamide. The progress curves were then plotted and compared to the appropriate enzyme control.[47]

4.5. Structure–activity relationship (SAR) analysis

We searched a number of commercially available small molecule databases and purchased analogs of the scaffolds identified in the HTS. Compounds 5140108, 6959933, 5237467, 7985301, 7988362, 6802623, 6836332, 6978945, and 5366302 were purchased from ChemBridge. Analogs of scaffold **14** were synthesized as previously described.[48] All other compounds used in the SAR analysis were purchased from Specs (R&D Chemicals). Each compound was tested in triplicate at 50 and 500 μM for its effect against Hst2 in the fluorigenic assay (1 μM Hst2, 100 μM Fluor de Lys-SIRT1 deacetylase substrate, and 160 μM NAD^+, 15 min reaction time). The resulting deacetylase activity for the three experiments was averaged and reported as a percentage relative to control wells containing no inhibitor. IC_{50} values were then measured for compounds that showed significant inhibition of Hst2 as exhibited by no activity at a compound concentration of 500 μM by the protocol described above.

4.6. Competition assay

Each of the identified inhibitor scaffolds was characterized with regard to its ability to compete with the Fluor de Lys-SIRT1

deacetylase substrate and NAD^+ for Hst2 binding. The fluorigenic assay described above was used with a fixed enzyme concentration of 1 μM. When competition with NAD^+ was being tested, the Fluor de Lys-SIRT1 deacetylase substrate was held at a constant concentration of 100 μM and the NAD^+ was titrated from 1/3 to 5× $K_{m\ NAD+}$ (5–80 μM). When competition with the Fluor de Lys-SIRT1 deacetylase substrate was being tested, the NAD^+ concentration was held constant at 160 μM and the Fluor de Lys-SIRT1 deacetylase substrate was titrated from 1/3 to 5× the $K_{m\ acetyl\text{-}lysine}$ (3–50 μM). The inhibitors were titrated from ~1/2 to several times their estimated K_i as indicated in the figure legend. The reaction time was 15 min, and each condition was tested in duplicate. The K_m, k_{cat}, and k_{cat}/K_m values were determined by direct fit of the data in SigmaPlot (Systat Software, Point Richmond, CA) to the Michaelis–Menten equation. The K_i and K_{is} (the slope and intercept inhibition constants, respectively) and the competition type were also determined by a direct fit in SigmaPlot to both partial and full competitive, non-competitive, uncompetitive and mixed competition models. Best-fit models were determined by several statistical methods including R^2, AICs, and Sy.x as well as empirical evaluation of α and β values.

4.7. Telomere silencing assay

Synthetic complete yeast media (SC) with or without 5-FOA was prepared with sirtuin inhibitors at indicated concentrations. Equal amounts of cells of yeast strains BY4741 (*MATa his3Δ1 leu2Δ0 met15Δ0 ura3Δ0*), YWD301 (*MATa his3Δ1 leu2Δ0 met15Δ0 ura3Δ0 sir2Δ::URA3*), FEP100-10 (*MATa leu2Δ1 ura3-52 can1-1 ade2Δ, URA3@TEL11L-XC*), and FEP132 (*MATa leu2Δ1 ura3-52 can1-1 ade2Δ sir2::kanMX4, URA3@TEL11L-XC*) were 10-fold serial diluted and spotted on indicated media. Pictures were taken after two days of growth at 30 °C.

Acknowledgments

The plasmid containing full length human SIRT1 (FL SIRT1) was a generous gift from Dr. David Sinclair (Harvard Medial School, Boston, MA), the plasmid containing isoform II of human SIRT2 was a generous gift from Danny Reinberg (Howard Hughes Medical Institute of NYU Medical School), and cambinol was a generous gift from Antonio Bedalov (Fred Hutchinson Cancer Center, Seattle, Washington). We thank Edward J Louis (University of Nottinghan, UK) for providing yeast strains FEP100-10 and FEP132; Nicola Toliday, Frank An, Stephanie Norton and Jason Burbank of the Broad Institute for help with HTS; Andre Isaacs for technical assistance and useful discussions; and Tom Beer and the Wistar Institute Proteomics Facility for assistance with mass spectrometry. This work was supported by the following grants from the National Institutes of Health: Grant CA107107 to R.M.; Grant AG031862 to R.M., W.D., and S.L.B.; and predoctoral fellowship T32-CA009171 to B.D.S. This project has been funded in part with Federal funds from the National Cancer Institute's Initiative for Chemical Genetics, National Institutes of Health, under Contract No. N01-CO-12400 and has been performed with the assistance of the Chemical Biology Platform of the Broad Institute of Harvard and MIT. The content of this publication does not necessarily reflect the views or policies of the Department of Health and Human Service, nor does mention of trade names, commercial products or organizations imply endorsement by the US Government.

Supplementary data

Supplementary data associated with this article can be found, in the online version, at doi:10.1016/j.bmc.2009.07.073.

References and notes

1. Imai, S.; Armstrong, C. M.; Kaeberlein, M.; Guarente, L. *Nature* **2000**, *403*, 795.
2. Landry, J.; Sutton, A.; Tafrov, S. T.; Heller, R. C.; Stebbins, J.; Pillus, L.; Sternglanz, R. *Proc. Natl. Acad. Sci. U.S.A.* **2000**, *97*, 5807.
3. Jackson, M. D.; Denu, J. M. *J. Biol. Chem.* **2002**, *277*, 18535.
4. Sauve, A. A.; Celic, I.; Avalos, J.; Deng, H.; Boeke, J. D.; Schramm, V. L. *Biochemistry* **2001**, *40*, 15456.
5. Kim, S.; Benguria, A.; Lai, C. Y.; Jazwinski, S. M. *Mol Biol Cell.* **1999**, *10*, 3125.
6. Kaeberlein, M.; McVey, M.; Guarente, L. *Genes Dev.* **1999**, *13*, 2570.
7. Lin, S. J.; Defossez, P. A.; Guarente, L. *Science* **2000**, *289*, 2126.
8. Brachmann, C. B.; Sherman, J. M.; Devine, S. E.; Cameron, E. E.; Pillus, L.; Boeke, J. D. *Genes Dev.* **1995**, *9*, 2888.
9. Tissenbaum, H. A.; Guarente, L. *Nature* **2001**, *410*, 227.
10. Rogina, B.; Helfand, S. L. *Proc. Natl. Acad. Sci. U.S.A.* **2004**, *101*, 15998.
11. Cohen, H. Y.; Miller, C.; Bitterman, K. J.; Wall, N. R.; Hekking, B.; Kessler, B.; Howitz, K. T.; Gorospe, M.; de Cabo, R.; Sinclair, D. A. *Science* **2004**, *305*, 390.
12. Boily, G.; Seifert, E. L.; Bevilacqua, L.; He, X. H.; Sabourin, G.; Estey, C.; Moffat, C.; Crawford, S.; Saliba, S.; Jardine, K.; Xuan, J.; Evans, M.; Harper, M. E.; McBurney, M. W. *PLoS ONE* **2008**, *3*, e1759.
13. Frye, R. A. *Biochem. Biophys. Res. Commun.* **1999**, *260*, 273.
14. Frye, R. A. *Biochem. Biophys. Res. Commun.* **2000**, *273*, 793.
15. Kim, E. J.; Um, S. J. *BMB Rep.* **2008**, *41*, 751.
16. Guarente, L. *Cold Spring Harb. Symp. Quant. Biol.* **2007**, *72*, 483.
17. Bitterman, K. J.; Anderson, R. M.; Cohen, H. Y.; Latorre-Esteves, M.; Sinclair, D. A. *J. Biol. Chem.* **2002**, *277*, 45099.
18. Schmidt, M. T.; Smith, B. C.; Jackson, M. D.; Denu, J. M. *J. Biol. Chem.* **2004**, *279*, 40122.
19. Luo, J.; Nikolaev, A. Y.; Imai, S.; Chen, D.; Su, F.; Shiloh, A.; Guarente, L.; Gu, W. *Cell* **2001**, *107*, 137.
20. Jackson, M. D.; Schmidt, M. T.; Oppenheimer, N. J.; Denu, J. M. *J. Biol. Chem.* **2003**, *278*, 50985.
21. Sauve, A. A.; Schramm, V. L. *Biochemistry* **2003**, *42*, 9249.
22. Vaziri, H.; Dessain, S. K.; Ng Eaton, E.; Imai, S. I.; Frye, R. A.; Pandita, T. K.; Guarente, L.; Weinberg, R. A. *Cell* **2001**, *107*, 149.
23. Jones, P. A.; Baylin, S. B. *Nat. Rev. Genet.* **2002**, *3*, 415.
24. Pruitt, K.; Zinn, R. L.; Ohm, J. E.; McGarvey, K. M.; Kang, S. H.; Watkins, D. N.; Herman, J. G.; Baylin, S. B. *PLoS Genet.* **2006**, *2*, e40.
25. Bedalov, A.; Gatbonton, T.; Irvine, W. P.; Gottschling, D. E.; Simon, J. A. *Proc. Natl. Acad. Sci. U.S.A.* **2001**, *98*, 15113.
26. Grozinger, C. M.; Chao, E. D.; Blackwell, H. E.; Moazed, D.; Schreiber, S. L. *J. Biol. Chem.* **2001**, *276*, 38837.
27. Heltweg, B.; Gatbonton, T.; Schuler, A. D.; Posakony, J.; Li, H.; Goehle, S.; Kollipara, R.; Depinho, R. A.; Gu, Y.; Simon, J. A.; Bedalov, A. *Cancer Res.* **2006**, *66*, 4368.
28. Lain, S.; Hollick, J. J.; Campbell, J.; Staples, O. D.; Higgins, M.; Aoubala, M.; McCarthy, A.; Appleyard, V.; Murray, K. E.; Baker, L.; Thompson, A.; Mathers, J.; Holland, S. J.; Stark, M. J.; Pass, G.; Woods, J.; Lane, D. P.; Westwood, N. J. *Cancer Cell.* **2008**, *13*, 454.
29. Tervo, A. J.; Kyrylenko, S.; Niskanen, P.; Salminen, A.; Leppanen, J.; Nyronen, T. H.; Jarvinen, T.; Poso, A. *J. Med. Chem.* **2004**, *47*, 6292.
30. Tervo, A. J.; Suuronen, T.; Kyrylenko, S.; Kuusisto, E.; Kiviranta, P. H.; Salminen, A.; Leppanen, J.; Poso, A. *J. Med. Chem.* **2006**, *49*, 7239.
31. Huhtiniemi, T.; Suuronen, T.; Rinne, V. M.; Wittekindt, C.; Lahtela-Kakkonen, M.; Jarho, E.; Wallen, E. A.; Salminen, A.; Poso, A.; Leppanen, J. *J. Med. Chem.* **2008**, *51*, 4377.
32. Trapp, J.; Jochum, A.; Meier, R.; Saunders, L.; Marshall, B.; Kunick, C.; Verdin, E.; Goekjian, P.; Sippl, W.; Jung, M. *J. Med. Chem.* **2006**, *49*, 7307.
33. Gey, C.; Kyrylenko, S.; Hennig, L.; Nguyen, L. H.; Buttner, A.; Pham, H. D.; Giannis, A. *Angew. Chem., Int. Ed.* **2007**, *46*, 5219.
34. Kahyo, T.; Ichikawa, S.; Hatanaka, T.; Yamada, M. K.; Setou, M. *J. Pharmacol. Sci.* **2008**, *108*, 364.
35. Chakrabarty, S. P.; Saikumari, Y. K.; Bopanna, M. P.; Balaram, H. *Mol. Biochem. Parasitol.* **2008**, *158*, 139.
36. Howitz, K. T.; Bitterman, K. J.; Cohen, H. Y.; Lamming, D. W.; Lavu, S.; Wood, J. G.; Zipkin, R. E.; Chung, P.; Kisielewski, A.; Zhang, L. L.; Scherer, B.; Sinclair, D. A. *Nature* **2003**, *425*, 191.
37. Napper, A. D.; Hixon, J.; McDonagh, T.; Keavey, K.; Pons, J. F.; Barker, J.; Yau, W. T.; Amouzegh, P.; Flegg, A.; Hamelin, E.; Thomas, R. J.; Kates, M.; Jones, S.; Navia, M. A.; Saunders, J. O.; DiStefano, P. S.; Curtis, R. *J. Med. Chem.* **2005**, *48*, 8045.
38. Trapp, J.; Meier, R.; Hongwiset, D.; Kassack, M. U.; Sippl, W.; Jung, M. *ChemMedChem.* **2007**, *2*, 1419.
39. Schuetz, A.; Min, J.; Antoshenko, T.; Wang, C. L.; Allali-Hassani, A.; Dong, A.; Loppnau, P.; Vedadi, M.; Bochkarev, A.; Sternglanz, R.; Plotnikov, A. N. *Structure* **2007**, *15*, 377.
40. Kiviranta, P. H.; Leppanen, J.; Kyrylenko, S.; Salo, H. S.; Lahtela-Kakkonen, M.; Tervo, A. J.; Wittekindt, C.; Suuronen, T.; Kuusisto, E.; Jarvinen, T.; Salminen, A.; Poso, A.; Wallen, E. A. *J. Med. Chem.* **2006**, *49*, 7907.
41. Kiviranta, P. H.; Leppanen, J.; Rinne, V. M.; Suuronen, T.; Kyrylenko, O.; Kyrylenko, S.; Kuusisto, E.; Tervo, A. J.; Jarvinen, T.; Salminen, A.; Poso, A.; Wallen, E. A. *Bioorg. Med. Chem. Lett.* **2007**, *17*, 2448.
42. Hirao, M.; Posakony, J.; Nelson, M.; Hruby, H.; Jung, M.; Simon, J. A.; Bedalov, A. *J. Biol. Chem.* **2003**, *278*, 52773.

43. Lara, E.; Mai, A.; Calvanese, V.; Altucci, L.; Lopez-Nieva, P.; Martinez-Chantar, M. L.; Varela-Rey, M.; Rotili, D.; Nebbioso, A.; Ropero, S.; Montoya, G.; Oyarzabal, J.; Velasco, S.; Serrano, M.; Witt, M.; Villar-Garea, A.; Inhof, A.; Mato, J. M.; Esteller, M.; Fraga, M. F. *Oncogene* **2009**, *28*, 781.
44. Mai, A.; Massa, S.; Lavu, S.; Pezzi, R.; Simeoni, S.; Ragno, R.; Mariotti, F. R.; Chiani, F.; Camilloni, G.; Sinclair, D. A. *J. Med. Chem.* **2005**, *48*, 7789.
45. Neugebauer, R. C.; Uchiechowska, U.; Meier, R.; Hruby, H.; Valkov, V.; Verdin, E.; Sippl, W.; Jung, M. *J. Med. Chem.* **2008**, *51*, 1203.
46. Posakony, J.; Hirao, M.; Stevens, S.; Simon, J. A.; Bedalov, A. *J. Med Chem.* **2004**, *47*, 2635.
47. Copeland, R. A. *Evaluation of Enzyme Inhibitors in Drug Discovery*; John Wiley & Sons: Hoboken, 2005.
48. Taylor, A. M.; Schreiber, S. L. *Org. Lett.* **2006**, *8*, 143.
49. Pryde, F. E.; Louis, E. J. *Embo J.* **1999**, *18*, 2538.
50. Nayagam, V. M.; Wang, X.; Tan, Y. C.; Poulsen, A.; Goh, K. C.; Ng, T.; Wang, H.; Song, H. Y.; Ni, B.; Entzeroth, M.; Stunkel, W. *J. Biomol. Screen.* **2006**, *11*, 959.
51. Marks, P. A.; Richon, V. M.; Breslow, R.; Rifkind, R. A. *Curr. Opin. Oncol.* **2001**, *13*, 477.
52. Piekarz, R. L.; Robey, R.; Sandor, V.; Bakke, S.; Wilson, W. H.; Dahmoush, L.; Kingma, D. M.; Turner, M. L.; Altemus, R.; Bates, S. E. *Blood* **2001**, *98*, 2865.
53. Sandor, V.; Bakke, S.; Robey, R. W.; Kang, M. H.; Blagosklonny, M. V.; Bender, J.; Brooks, R.; Piekarz, R. L.; Tucker, E.; Figg, W. D.; Chan, K. K.; Goldspiel, B.; Fojo, A. T.; Balcerzak, S. P.; Bates, S. E. *Clin. Cancer Res.* **2002**, *8*, 718.
54. Zhao, K.; Chai, X.; Clements, A.; Marmorstein, R. *Nat. Struct. Biol.* **2003**, *10*, 864.